Notes

Inner Product of RGB Unit Vectors for Detecting Color Transition. Application to Feedback-based Flow Ratiometric Titration

Naoya KAKIUCHI,* Junya OCHIAI,** Masaki TAKEUCHI,*,**,*** and Hideji TANAKA*,**,***†

* *Graduate School of Pharmaceutical Sciences, Tokushima University, 1-78-1 Shomachi, Tokushima 770-8505, Japan*

** *Faculty of Pharmaceutical Sciences, Tokushima University, 1-78-1 Shomachi, Tokushima 770-8505, Japan*

*** *Institute of Biomedical Sciences, Tokushima University, 1-78-1 Shomachi, Tokushima 770-8505, Japan*

† To whom correspondence should be addressed.

E-mail: h.tanaka@tokushima-u.ac.jp

Abstract

The inner product (IP) of RGB unit vectors' approach for detecting color transition has further been applied to a feedback-based flow ratiometric titration, including nonaqueous titration. While the flow ratio of titrand/titrant containing an indicator was varying, the video image of the merged solution was taken with a digital microscope downstream. The indicator's color was converted to an RGB unit vector. The change in IP between vectors was used for determining the equivalence point. The concept was successfully applied to the determinations of drug and vinegar samples with reasonable throughput rate (> 18 s/titration) and precision (RSD < 4.4%).

Keywords Inner product, RGB unit vector, hue, flow ratiometry, titration, digital microscope

Introduction

With the widespread use of digital cameras and smartphones, the number of reports on image-based detection using these devices has been increasing greatly. The examples of the earliest studies were Li^+ sensing by a plastic film and paper optodes,[1] and Al^{3+} and Fe^{3+} determinations using a chromogenic reagent;[2] examples of very recent studies include the applications to flow analysis,[3] drop-based analysis,[4] photonic gel sensing,[5] paper-based sensing[6-8] and so on. Soda and Bakker[9] correlated the image-based absorbance with the spectrophotometrically determined absorbance. As for applying digital image-based colorimetry to titration, Araújo *et al*.[10-15] determined indicator's color transition based on RGB and/or Hue values. Recently, Ruttanakorn *et al*. proposed an RGB linear segment titration curve technique for equivalence point detection.[16] However, these methods needed to select an appropriate color specification value (*i.e.*, R, G, B, or hue value) prior to the analysis.

In our Rapid Communication,[17] a new concept for detecting color transition based on an inner product (IP) of RGB unit vectors was proposed. The concept was validated by applying to a fixed triangular wave-controlled flow ratiometric titration.[18]

In the present study, the method is further applied to aqueous and nonaqueous titrations of drug and vinegar samples by a feedback-based flow ratiometry.[18-21] Drugs listed in the 18th Japanese Pharmacopoeia[22] and commercial vinegar samples were selected as target samples.

Experimental

Reagents and samples

The reagents used in the present study were of analytical reagent grade purchased from

Kanto Chemicals (Tokyo), Nacalai Tesque (Kyoto), or Fujifilm Wako Pure Chemical Co. (Osaka). Bulk powder of isoniazid (ISCOTIN®), 250 mg tablet of probenecid (BENECID®), and fine granules of 50% sulpiride were purchased from Daiichi Sankyo Co., Kaken Pharmaceutical Co., and Kyowa Pharmaceutical Industry Co., respectively. Fine granules of 4% furosemide (Lasix®) and 100 mg tablet of ibuprofen (BRUFEN®) were purchased from Nichi-Iko Pharmaceutical Co. Figures S1A – E (Supporting Information) show the structural formula of the drugs. Grain, apple, and rice vinegar samples were purchased at local markets in Tokushima, Japan. Sartorius Arim 611DI grade deionized water was used throughout.

Method

Figure 1 shows the schematic diagram of the present system. Acid flow rate F_A (= kV_c, where k is a proportional constant) was varied with control signal V_c supplied from a laptop computer PC *via* an A/D-D/A converter. A base solution containing an indicator was aspirated at a flow rate of $F_T - F_A$, where F_T means the total flow rate. The merged solution was introduced to a specially fabricated detector,[17] where a digital video image of the solution flowing through a quartz flow cell (optical path length: 1 mm) was taken with a digital microscope. The image data were acquired in PC using the OpenCV Library (ver. 2.4.13). An in-house program written in Visual Basic .NET was used for conducting the above processes automatically.

The RGB unit vector $\vec{v}$ is expressed by Eq. (1).

$$\vec{v} = (r, g, b), \quad r \text{ (or } g, b) = \frac{R^2 \left(\text{or } G^2, B^2\right)}{\sqrt{R^2 + G^2 + B^2}} \qquad (1)$$

An inner product (IP_i) of the first and the i^{th} image vector ($\vec{v_1}$ and $\vec{v_i}$, respectively) was

obtained by the following equation.[17]

$$IP_i = r_1 r_i + g_1 g_i + b_1 b_i \qquad (2)$$

IP_i is 1 or <1 if the two vectors are the same or different, respectively. Therefore, drastic IP_i change around the equivalence point can be used as a criterion for the indicator's color transition.

The principle of feedback-based flow ratiometry was reported before by Tanaka *et al.,*[18] and is explained in Fig. S2 (Supporting Information). In the present study, IP instead of detector output voltages[18-21,23,24] was used for the equivalence point detection. The calibration curve was obtained by plotting V_E^{-1} against the base concentration C_B^{-1} or the reciprocal of the acid concentration C_A, where V_E means the V_c that gives the equivalence composition.

$$\frac{1}{V_E} = \frac{n_A k C_A}{n_B F_T C_B} + \frac{k}{F_T} , \qquad (3)$$

where n_A and n_B are the valences of the acid and the base, respectively.

Results and Discussion

Prior to the application to drug and vinegar analyses, titrations of HCl *vs.* NaOH, CH_3COOH *vs.* NaOH, H_3PO_4 (1st) *vs.* NaOH, and NH_3 *vs.* HCl, with Bromothymol Blue (BTB), Phenolphthalein (PP), Thymolphthalein (TP), and Bromocresol Green (BCG) as respective indicators, were examined by the present method. Linear calibration curves ($r^2 > 0.998$) were

obtained in the ranges of 0.030 – 1.0, 0.030 – 0.75, 0.030 – 0.30, and 0.050 – 1.0 mol dm^{-3}, respectively. For example, Fig. S3 (Supporting Information) shows the result for the titration of 0.1 mol dm^{-3} NaOH with 0.1 mol dm^{-3} HCl.

Figures 2A, B, and C show the temporal profiles of V_c, IP, and hue, respectively, for the nonaqueous titration of 20 mmol dm^{-3} sulpiride in acetic acid containing 2.0 mmol dm^{-3} Crystal Violet (CV). The titrant was 20 mmol dm^{-3} $HClO_4$ in acetic acid. The scan direction of V_c was changed from upward to downward when IP reached IP_{set} (0.7: equivalence IP level[17]) at 27.9, 65.4, and 103.2 s, and *vice versa* at 46.8 and 84.3 s. The V_E, determined by averaging the most recent V_c maximum (V_H) and minimum (V_L) values,[18] was 2.76 ± 0.02 V (n = 4). The hue value also changed considerably from 250° (blue) to 30° (orange) *via* 360° (= 0°) (red). The change in hue value would, however, be small if an indicator having a narrow transition interval in the hue ring, such as Methyl Red for aqueous titration, were used. Figure 2D shows the titration curve, where IP (Fig. 2B) was plotted against V_c (Fig. 2A). In contrast to the previous fixed triangular wave-controlled approach (scan range of 0 – 5 V),[17] the present feedback-based method could limit the range by 43%, resulting in a higher throughput rate of 19.1 ± 0.3 s/titration (n = 4). In principle, the color change in the downward V_c scan must trace the change in the upward V_c scan in reverse. However, no data was sensed during one sampling period (0.1 s) between a and b in Figs. 2B–D. Similar tendencies were observed for other drugs tested. The reason for this rapid transition is not apparent at present.

Table 1 summarizes the calibration curves for various drugs, showing acceptable ranges and linearity ($r^2 > 0.996$). The calibration curves are also graphically displayed in Figs. S4A – E (Supporting Information). Temporal profiles and titration curve, such as those in Fig. 2, for various concentrations of sulpiride, for example, are shown in Fig. S5 (Supporting Information).

Commercial vinegar samples were analyzed by the present method. The results are listed in Table 2, together with those obtained by the official batch method.[25] Analytical values met

the regulation of the Japanese Agricultural Standards[25] (JAS) and the U.S. Food and Drug Administration (FDA),[26] where the minimum acidity of the vinegar is specified as 4.0%. No significant differences (95% confidence level of Student's *t*-test) were found between the proposed method and the official method. The relative error was as low as ± 1%. The precision (RSD = 0.6 – 3.2%) is comparable to the previous study (RSD = 0.5 – 1.7%) using a LED-photodiode detector.[23]

Acknowledgments

The present study was partly supported by a Grant-in-Aid for Scientific Research (C) (21K0512700) from the Japan Society for the Promotion of Sciences (JSPS).

Supporting Information

The structural formula of drugs are shown in Fig. S1. The principle of feedback-based flow ratiometry is shown in Fig. S2. The results for the titration of 0.1 mol dm^{-3} HCl with 0.1 mol dm^{-3} NaOH are shown in Fig. S3. Calibration curves for drugs are shown in Fig. S4. Temporal profiles of V_c, IP and hue, and titration curves at various concentrations of sulpiride are shown in Fig. S5. These materials are available free of charge on the Web at http://www.jsac.or.jp/analsci/.

References

1. E. Hirayama, T. Sugiyama, H. Hisamoto, and K. Suzuki, *Anal. Chem.*, **2000**, *72*, 465; https://doi.org/10.1021/ac990588w.

2. N. Maleki, A. Safavi, and F. Sedaghatpour, *Talanta*, **2004**, *64*, 830; https://doi.org/10.1016/j.talanta.2004.02.041.

3. K. Danchana and V. Cerdá, *Talanta*, **2020**, *216*, 120977; https://doi.org/10.1016/j.talanta.2020.120977.

4. S. Apichai, K. Thajee, W.Wongwilai, S. Wangkarn, P. Paengnakorn, C. Saenjum, and K. Grudpan, *Talanta*, **2019**, *201*, 226; https://doi.org/10.1016/j.talanta.2019.04.014.

5. H. Park, Y. G. Koh, W. Lee, *Sens. Actuators B Chem*., **2021**, *345*, 130359; https://doi.org/10.1016/j.snb.2021.130359.

6. K. Sankar, D. Lenisha, G. Janaki, J. Juliana, R. S. Kumar, M. C. Selvi, and G. Srinivasan, *Talanta*, **2020**, *208*, 120408; https://doi.org/10.1016/j.talanta.2019.120408.

7. H. Sharifi, J. Tashkhourian, and B. Hemmateenejad, *Anal. Chim. Acta*, **2020**, *1126*, 114; https://doi.org/10.1016/j.aca.2020.06.006.

8. A. Lert-itthiporn, P. Srikritsadawong, N. Choengchan, *Talanta*, **2021**, *221*, 121574; https://doi.org/10.1016/j.talanta.2020.121574.

9. Y. Soda and E. Bakker, *ACS Sens*., **2019**, *4*, 3093; https://pubs.acs.org/doi/10.1021/acssensors.9b01802.

10. E. da N. Gaiao, V. L. Martins, W. da S. Lyra, L. F. de Almeida, E. C. da Silva, and M. C. U. Araújo, *Anal. Chim. Acta*, **2006**, *570*, 283; https://doi.org/10.1016/j.aca.2006.04.048.

11. A. R. Tórres, W. da Silva Lyra, S. I. E. de Andrade, R. A. N. Andrade, E. C. da Silva, M. C. U. Araújo, and E. da N. Gaião, *Talanta*, **2011**, *84*, 601; https://doi.org/10.1016/j.talanta.2011.02.002.

12. M. B. Lima, S. I. E. Andrade, I. S. Barreto, L. F. Almeida, and M. C. U. Araújo, *Microchem.*

J., **2013**, *106*, 238; https://doi.org/10.1016/j.microc.2012.07.010.

13. S. I. E. Andrade, M. B. Lima, I. S. Barreto, W. S. Lyra, L. F. Aleida, M. C.U. Araújo, and E. C. Silva, *Microchem. J.*, **2013**, *109*, 106; https://doi.org/10.1016/j.microc.2012.03.029.
14. M. A. Domínguez, P. H. G. D. Diniz, M. S. D. Nezio, M. C. U. de Araújo, and M. E. Centurión, *Microchem. J.*, **2014**, *112*, 104; https://doi.org/10.1016/j.microc.2013.09.008.
15. L. A. Siqueira, I. S. Nunes, P. L. Almeida Junior, W. S. Lyra, R. A. N. Andrade, M. C. U. Araújo, L. F. Almeida, and R. A. C. Lima, *Microchem. J.*, **2017**, *133*, 593; https://doi.org/10.1016/j.microc.2017.04.041.
16. K. Ruttanakorn, N. Phadungcharoen, W. Laiwattanapaisal, A. Chinsriwongkul, and T. Rojanarata, *Talanta*, **2021**, *233*, 122602; https://doi.org/10.1016/j.talanta.2021.122602.
17. N. Kakiuchi, J. Ochiai, M. Takeuchi, and H. Tanaka, *Anal. Sci.*, **2021**, *37*, 3; https://doi.org/10.2116/analsci.20C015.
18. H. Tanaka, P. K. Dasgupta, and J. Huang, *Anal. Chem.*, **2000**, *72*, 4713; https://doi.org/10.1021/ac000598t.
19. P. K. Dasgupta, H. Tanaka, and K. D. Jo, *Anal. Chim. Acta*, **2001**, *435*, 289; https://doi.org/10.1016/S0003-2670(01)00864-9.
20. P. K. Dasgupta and K. D. Jo, *Electroanalysis*, **2002**, *14*, 1383; https://doi.org/10.1002/1521-4109(200211)14:19/20%3C1383::AID-ELAN1383%3E3.0.CO;2-I
21. K. D. Jo and P. K. Dasgupta, *Talanta*, **2003**, *60*, 131; https://doi.org/10.1016/s0039-9140(03)00114-0.
22. The Japanese Pharmacopoeia, 18th ed., **2021**, The Ministry of Health, Labor and Welfare, Tokyo.
23. N. Kakiuchi, A. Miyazaki, A. Fujikawa, M. Takeuchi, and H. Tanaka, *J. Flow Injection Anal.*, **2017**, *34*, 11; https://doi.org/10.24688/jfia.34.1_11.
24. J. Ochiai, S. Oka, T. Hirasaka, E. Tomiyama, H. Kubo, K. Okamoto, M. Takeuchi, and H.

Tanaka, *Anal. Sci.*, **2020**, *36*, 703; https://doi.org/10.2116/analsci.19P401.

25. JAS, “Japanese Agricultural Standard for Brewed Vinegar”, **2019**, Ministry of Agriculture, Forestry and Fisheries, Japan.

26. Compliance Policy Guide Sec. 525.825 “Vinegar, Definitions - Adulteration with Vinegar Eels”, **1995**, U.S. Food and Drug Administration.

Table 1 Calibration curves of various drugs

Titrand	Titrant	Indicator[a]	Linear range / mmol dm^{-3}	r^2
Isoniazid	$HClO_4$[b]	PNB	2.5 – 270	0.999
Furosemide	NaOH[c]	BTB	0.6 – 12	0.996
Ibuprofen	NaOH[d]	PP	12 – 120	0.998
Probenecid	NaOH[e]	PP	14 – 140	0.999
Sulpiride	$HClO_4$[f]	CV	5.4 – 54	0.996

[a] PNB: *p*-Naphtholbenzein, BTB: Bromothymol Blue, PP: Phenolphthalein, CV: Crystal Violet. Isoniazid, sulpiride, and $HClO_4$ were respectively dissolved in acetic acid; furosemide was dissolved in *N*,*N*-dimethylformamide; ibuprofen and probenecid were respectively dissolved in ethanol. NaOH was dissolved in water. Titrant concentration in mmol dm^{-3}: b, 20; c, 10; d, 50; e, 100; f, 20.

Table 2 Quantification of vinegar samples

Titrand	Titrant[a]	Indicator	Concentration,%		Relative error[b], %
			Present method	Official method	
Grain vinegar	NaOH	PP	4.62 ± 0.03	4.62 ± 0.02	0
Apple vinegar	NaOH	PP	4.74 ± 0.15	4.80 ± 0.01	− 1.0
Rice vinegar	NaOH	PP	4.93 ± 0.13	4.88 ± 0.01	1.0

(n = 3)

[a] The concentration was 50 mmol dm^{-3}.

[b] Relative error = (reference value − present value)/(reference value) × 100%, where reference and present values mean the concentrations obtained by the official and the present methods, respectively.

Figure Captions

Fig. 1 Flow system

P_1 and P_2, peristaltic pump (GILSON, Minipuls 3, MP-2, USA); DM, digital microscope (UMTELE Co., YPC-X02, China); PC, laptop computer (Hewlett Packard, HP-ProBesk 430 G3, USA) with an A/D-D/A converter (Contec, AIO-16082 GY-USB, Japan); V_c, control voltage; W, waste. F_A (0 – 1.15 cm^3 min^{-1}), F_B ($F_T - F_A$) and F_T (1.20 cm^3 min^{-1}) are acid, base and total flow rates, respectively. Polytetrafluoroethylene tubing (1.60 mm o.d., 0.5 mm i.d.) and Pharmed® tubing (3.68 mm o.d., 0.51 mm i.d.) were used as the conduit and pump tubing, respectively. No mixing reactor was used because the rollers of P_2 actively facilitated the mixing.

Fig. 2 Flow signals for titration of 20 mmol dm^{-3} sulpiride. Sampling frequency: 10 Hz. (A) Control voltage, V_c. V_c scan rate: 150 mV s^{-1}. (B) Inner product (IP) of two RGB unit vectors for the first image and the i^{th} images. (C) Hue value. (D) Titration curve. The color for each data plot in Fig. 2B, C and D indicates the indicator's color. Horizontal and vertical dashed lines show IP_{set} and V_E, respectively.

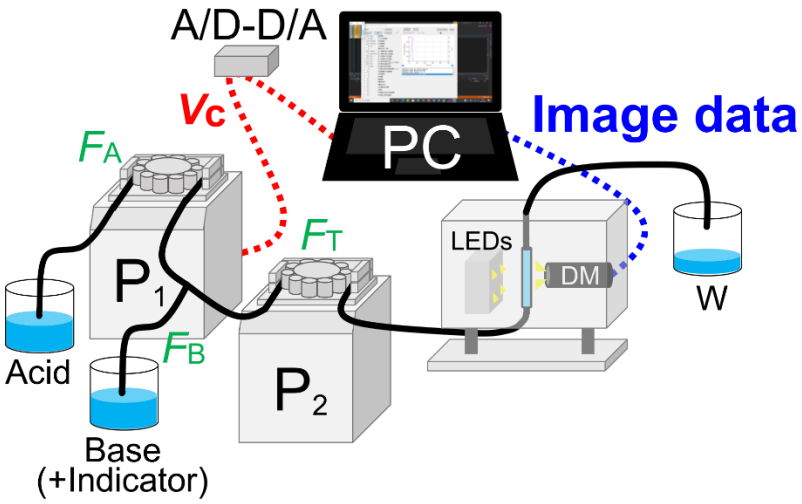
A/D-D/A
Vc
PC
Image data
FA
FT
LEDs
DM
W
P1
P2
FB
Acid
Base
(+Indicator)

Fig. 1

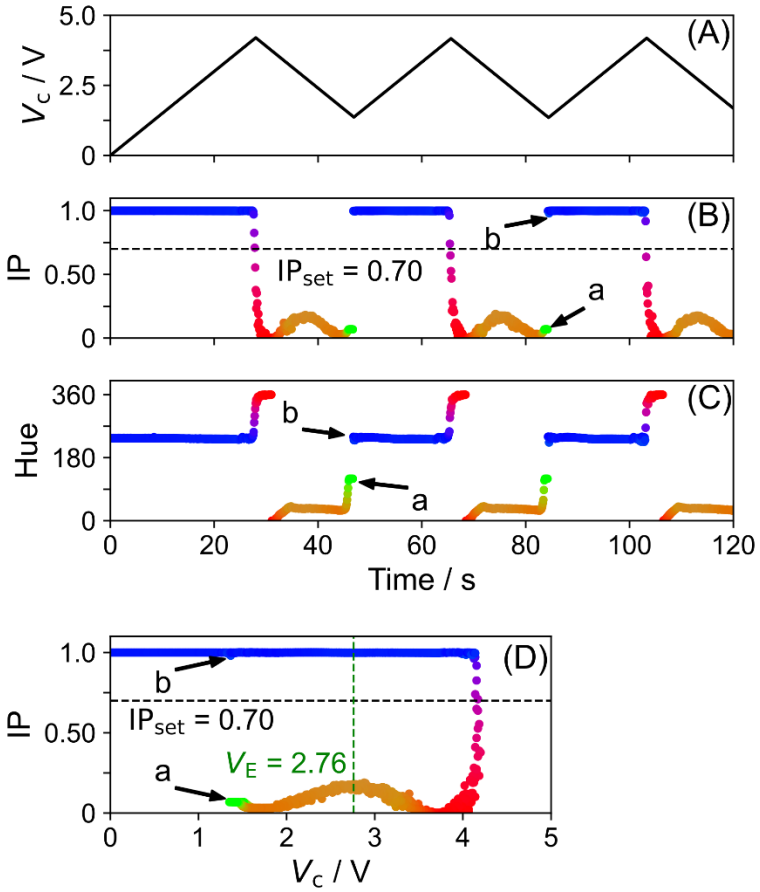
(A)
V_c / V
5.0
2.5
0
(B)
IP
1.0
0.50
0
IP_{set} = 0.70
b
a
(C)
Hue
360
180
0
b
a
0
20
40
60
80
100
120
Time / s
(D)
IP
1.0
0.50
0
b
IP_{set} = 0.70
a
V_E = 2.76
0
1
2
3
4
5
V_c / V

Fig. 2

Graphical Index